R. P. Dring
Supervisor.
Gas Turbine Technology

M. F. Blair
Research Engineer.
Mem. ASME

H. D. Joslyn
Research Engineer.

United Technologies Research Center
East Hartford, Conn.

An Experimental Investigation of Film Cooling on a Turbine Rotor Blade

Film cooling has been studied on the rotor blade of a large scale (low speed) model of a high pressure turbine first stage. Film coolant was discharged from single holes on the pressure and suction surfaces of the airfoil. For each blowing site the coolant to free stream mass flux ratio and density ratio were varied from 0.5 to 1.5 and from 1.0 to 4.0 respectively. Both surface flow visualization and local film cooling adiabatic effectiveness data were obtained. The observation was made that although it can have a strong radial component, the trajectory of the film coolant was very insensitive to coolant flow conditions. The existence of the radial component of the film coolant trajectory was found to have a strong impact on the nature of the effectiveness distribution. The data have been compared with data taken by other investigators on flat surfaces and in plane cascades. Agreement between the flat plate data and the suction surface data was reasonably good. However, the pressure surface results showed a much faster decay of the effectiveness than did the flat plate data due to effects thought to be related to both curvature and radial flow.

Introduction

With the evolution of gas turbine cycles with higher turbine inlet temperatures has come the need for increasingly effective means of cooling the turbine airfoils. One such cooling technique currently receiving wide application is film cooling. During recent years, many parameters affecting film cooling have been intensively studied. A survey of work up to 1971 has been published by Goldstein [1]. Although the bulk of the discussion is related to slot injection, there was some discussion of isolated hole injection. Ericksen [2] investigated film cooling behind a row of inclined holes, and among other things found that the effect of Reynolds number was relatively small. A simple analytical model of the effectiveness pattern produced by a jet has been published by Ericksen, et al., [3]. Pedersen [4] also looked at a row of inclined holes including mainstream to coolant density ratio as a prime variable. This permitted him to vary the mass and momentum flux ratios independently. He presented a correlation of his results including the effects of all these variables. Liess, et al., [5] examined the effects of free stream acceleration and Mach number and found them to be small. Lander, et al., [6] measured film cooling effectiveness on a first vane cascade in an attempt to include realistic geometry and flow conditions (including free stream turbulence). Finally, Muska, et al., [7] confirmed the additive nature of the effectiveness of multiple rows of film cooling holes. Although film cooling has been applied to many turbine rotor blades, there is no background at all on the impact of rotation and radial flow on the film coolant trajectory or film effectiveness.

There are, however, numerous aerodynamic mechanisms present in a turbine rotor blade passage which can give rise to radial flows. Aside from end effects such as tip leakage and end wall boundary layer vortices there are the following: three-dimensional inviscid flow (both irrotational and rotational) and three-dimensional boundary layer flow on the airfoils. With film cooling the potential exists for an additional effect due to rotation since the density of the coolant fluid can be as high as three times that of the free stream fluid. In the absence of any information on these effects they are ignored in the typical design system. Historically it has been assumed that the radial velocity in the film is zero. Any shortcoming of this approach has been compensated for by calibrating the design system on engine experience.

Description of Test Equipment and Techniques

Test Equipment. The experimental program was carried out in a 5 ft dia rotating rig with a 1½ stage turbine model having a 0.8 hub/tip ratio. This is a low speed facility which draws ambient air (from out-of-doors) through a series of screens and flow straighteners prior to reaching the inlet guide vanes. The axial chords of the airfoils in each row of the turbine model are all approximately 6 in. (0.15 m) or approximately five times engine scale. At a typical running condition, the axial flow velocity in the test section is 75 ft/s (23 m/s) and the shaft speed is 405 rpm. Airfoil Reynolds numbers are approximately 5.6×10^5 which is typical of high pressure turbine airfoils. Because the rig also has velocity triangles typical of those of a high

Contributed by the Gas Turbine Division and presented at the Gas Turbine Conference and Exhibit and Solar Energy Conference, San Diego, California, March 12–15, 1979 of THE AMERICAN SOCIETY OF MECHANICAL ENGINEERS. Manuscript received at ASME Headquarters December 8, 1979. Paper No. 79-GT-32.

pressure turbine, it provides an excellent simulation of the centrifugal and Coriolis effects as they would occur in the boundary layers of an actual engine scale turbine airfoil. The two-dimensional aerodynamic design of the rotor and its radial stacking are typical of current turbine designs.

For these film cooling tests coolant to free stream density ratios from 1.0 to 4.0 were produced using mixtures of air and sulfur hexafluoride, SF_6 (molecular weight = 146) as the coolant fluid. A trace amount of ammonia was included in some tests for flow visualization purposes. As previously mentioned, the turbine free stream fluid was air at ambient conditions. The coolant mixtures were heated above the free stream temperature and adiabatic effectiveness was determined by measuring the free stream and coolant temperatures and the adiabatic recovery temperature distribution on the airfoil surface with a matrix of thermocouples downstream of each blowing site.

Two coolant hole locations were chosen for this study, one at midspan and ten percent axial chord on the suction surface and one at midspan and 16 percent axial chord on the pressure surface. These holes are sufficiently far aft so as to be relatively uninfluenced by the details of the leading edge flow, and yet far enough forward so as to be uninfluenced by the suction surface endwall vortices and by the strong acceleration toward the trailing edge on the pressure surface. At the suction surface location the local flow velocity is roughly five times that at the pressure surface location. It was expected that at the low free stream velocity locations, such as on the pressure surface, that the radial flow effects would be much more strongly felt than on the high velocity locations, such as on the suction surface.

A flow metering system consisting of four calibrated glass rotameters was assembled to provide precise flows of the film coolant mixture to the blowing sites at various coolant blowing rates, M, and various coolant to free stream fluid density ratios, R. The error expected from these meters is ±1½ percent on the average and ±3 percent maximum.

Blade Pressure Distribution Measurements. In order to set the coolant flow rate, it was necessary to know the free stream velocity at each blowing site. For this purpose the rotor blade midspan pressure distribution was measured at a nominal (design) value of (C_x/U_m) of 0.78. The data taken included (1) airfoil midspan surface pressures at twenty-two locations around the perimeter of the blade, (2) rotor inlet relative total pressure at midspan (from a rotor mounted Kiel probe) and (3) rotor exit tip static pressure measured on the rotor casing. The rotating frame pressures were measured using a rotor-mounted scanivalve and transducer.

When comparing measured pressures to computed pressure distributions, it is convenient to use a pressure coefficient based on the blade exit midspan static pressure ($P2$) as a reference pressure and the difference between the inlet total pressure and the midspan exit static pressure as a normalizing pressure difference ($PT1$-$P2$). It was found in all cases that the measured pressure surface maximum pressures were slightly lower than one would expect from the measured rotor inlet total pressures. This difference, however, is only about one percent of the rotor exit relative dynamic pressure. This effect is probably related to radial flows in the rotor channel shifting the location of the high and the low total pressure fluid between the inlet total pressure probe (which is at the rotor leading edge plane) and the 30 percent chord location where the pressure surface pressure is near its maximum. In all cases the total pressure that was inferred from the pressure surface was used in evaluating the airfoil distributions. The midspan exit static pressure was determined by applying a correction to the static pressure measured on the rotor exit tip casing. This correction was based on the assumption of free-vortex flow. This is a very small correction (roughly one percent of the rotor exit relative dynamic pressure) and hence the slight inaccuracy associated with the assumption of free-vortex flow is negligible. The results are shown as data points in Fig. 1.

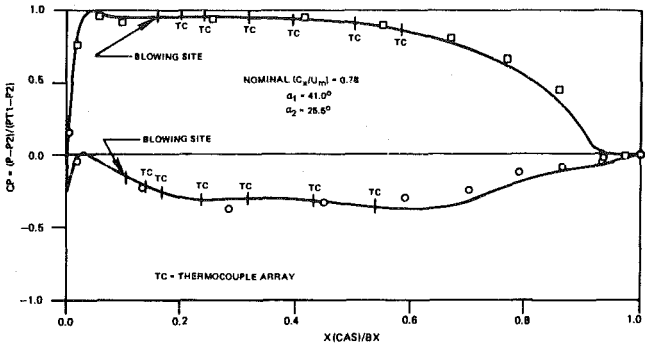

Fig. 1 Rotor midspan pressure distribution

The computed curve in Fig. 1 is based on an inviscid potential flow calculation [8]. The inlet and exit flow angles (α_1 and α_2 measured from tangential) were adjusted to give best agreement with the measurements. The predicted trailing edge stagnation point singularity has been eliminated in favor of the more physically realistic trailing edge condition of a base pressure equal to the downstream static pressure ($C_p = 0$). This affects the pressure distribution over less than the aft-most ten percent of the airfoil, i.e., X/BX from 0.9 to 1.0.

In general the measured and computed pressure distributions are in excellent agreement. The agreement is especially good in the leading edge region where the film coolant blowing sites are located. The suction and pressure surface blowing sites are 10 and 16 percent axial chord respectively from the leading edge as indicated in Fig. 1. From these results it has been determined that the local surface flow velocities at the suction and pressure surface blowing sites are (as a fraction of rotor midspan wheel speed) 2.05 and 0.40 respectively at the design point value of (C_x/U_m). This corresponds to 196 and 38 ft/s at a typical running condition of 405 rpm. The error expected in these velocities is ±1 percent for the suction surface and ±5 percent for the pressure surface. These results were used to compute the various film coolant mass flow rates required to achieve the desired values of the coolant to free stream mass flux ratio, M and the coolant to free stream density ratio, R.

Flow Visualization Tests. The first phase of the film cooling test program consisted of a series of flow visualization tests employing ammonia and Ozalid paper. The objective of these tests was to qualitatively determine the nature of the film coolant footprint on the airfoil surface downstream of each blowing site for the full range of density ratios, R, and blowing rates, M, to be studied in the program. These flow visualization film cooling patterns could then be employed to determine the effectiveness instrumentation arrays.

Both the flow visualization and effectiveness test airfoils were fabricated by casting duplicates of machined aluminum rotor blades (B_x = 6.34 in., 16.6 cm) with rigid urethane foam. This particular foam material was selected for its extremely low thermal conductivity (0.02

Nomenclature

B_x = airfoil axial chord
C_x = axial component of flow velocity
D = discharge hole diameter
I = momentum flux ratio: $(\rho V^2)_c/(\rho V^2)_f$
M = mass flux ratio: $(\rho V)_c/(\rho V)_f$
R = density ratio: (ρ_c/ρ_f)
Re_D = blowing site Reynolds number: $(\rho_f V_f D/\mu)$
S = surface arc length
T = temperature
U_m = wheel speed at midspan
V = flow velocity
X = axial distance
β = angle between the discharge hole axis and a plane tangent to the airfoil surface
δ^* = boundary layer displacement thickness
η = cooling effectiveness: $(T_s - T_f)/(T_c - T_f)$
ρ = fluid density
μ = fluid absolute viscosity

Subscripts

c = coolant
f = free stream
s = surface

to 0.03 Btu/hr ft °F). While this property is unimportant to the flow visualization tests it is important in the measurement of local film effectiveness [9].

The foam airfoils were fabricated using the following procedure. First holes (⅛ in. dia, 3.2 mm) were drilled into the aluminum rotor blade. The hole locations are known to within 0.3 percent of axial chord which is a relatively small fraction of the hole diameter. Each hole is inclined at an angle of 30 deg to the surface. The plane of each hole was set such that the axis of the hole is tangent to a cylindrical surface intersecting the airfoil at the location. The result is that all of the holes are oriented in the streamwise direction with no radial component. Next a hydrocalic cement mold was cast around the metal blade with drill rods inserted in the coolant holes. Finally the rigid foam was cast in the concrete mold producing a precise copy of the original metal blade.

With the flow visualization airfoils mounted on the rotor and a piece of Ozalid paper mounted on the airfoil surface behind the blowing site the rig was brought up to the desired running conditions of through flow velocity (C_x) and midspan wheel speed (U_m) such that the nominal design point velocity triangles (i.e., C_x/U_m) were obtained. The flow metering device was then connected to one of the blowing sites and the air and sulfur hexafluoride (SF_6) flow rates were adjusted until the desired coolant to free stream density ratio R, and coolant to mainstream mass flux ratio, M, were obtained. When the flow was established, a trace amount of ammonia was introduced into the film coolant flow. The amount of ammonia was always less than one percent of the total coolant mass flow so it had a negligible effect on both the R and M ratios. A strobe light triggered with a once per revolution pulse from the rotor shaft was used to observe the flow trace on the ozalid paper. After a trace of suitable darkness had been achieved, the ammonia was turned off and the lines were flushed with ammonia free flow. The flow metering device was then connected to the rotary union channel leading to the other blowing site and the process was repeated.

Figure 2 is a typical example of the flow visualization results. Traces are shown for a low M ratio and for both the suction and pressure surface blowing sites at nominal density ratios, R of 1 and 4. In all cases the suction surface film coolant trajectory is narrow, straight and has only a slight radial displacement. The pressure surface trajectory on the other hand is much wider, displays noticeable curvature, and has a strong radial displacement (roughly 30 deg radially outward). In comparing the various traces, it must be kept in mind that the relative darkness of each trace is primarily a function of how long the ammonia was allowed to flow. It should not be related directly to film coolant effectiveness. The trace width is also a function of the ammonia flow time but to a much lesser degree.

In order to gain additional insight into the flow mechanisms occurring in the experiment, a very small amount of pure ammonia was passed through both blowing sites. It was expected that this would indicate the nature of the flow over the blade in the absence of film coolant discharge. The results were virtually identical to those of Fig. 2. This indicates that it is unlikely that the pressure surface radial flow is due to a three-dimensional boundary layer since if this were the case the flow visualization trace direction would be expected to change somewhat when going from very low to very high blowing rates as the coolant jet penetrated the free stream. Such a change in direction was not observed to occur. The suction and pressure surface film coolant trajectories appear to be simply following the three-dimensional inviscid flow over the airfoil. Without a fully three-dimensional rotating frame cascade flow analysis, it is difficult to say with certainty what aspects of the rotor design have produced the radial flows.

Effectiveness Measurement. Upon completion of the flow visualization tests, the fabrication of two instrumented effectiveness airfoils was initiated. The two airfoils were cast using the previously discussed low thermal conductivity urethane foam. One airfoil had the suction surface blowing site (at ten percent chord) and the other airfoil had the pressure surface blowing site (at 16 percent chord). These airfoils were cast with thermocouples (TC's) mounted internally in the film coolant supply lines so that the coolant temperature could be measured immediately prior to ejection at the airfoil surface. Airfoil surface TC arrays located downstream of each blowing site were determined on the basis of the flow visualization results. The streamwise positioning, the radial extent and the locations where TC's were concentrated were all based on the flow visualization results. Figure 3 shows the array on the airfoil with the pressure surface blowing site. Six rows of hole pairs (two for each TC) can be seen with 8 to 12 thermocouples mounted in each row. The TC rows have been shown in relation to the airfoil pressure distribution in Fig. 1. One mil (0.025 mm) dia chromel-alumel thermocouples were welded to three mil (0.075 mm) dia chromel-alumel wires in internal chambers on each airfoil. These heavier leads then passed out of the airfoils through the hub attachment buttons. When all the TC's were mounted, a thin coat of varnish was applied to the test surfaces to hold the TC's firmly in position and to restore the surface smoothness.

For the effectiveness tests the "coolant" fluid passed from the calibrated metering system through the rotary union, through an electrical heater, and into each airfoil. The heater was used to bring the coolant gas flow to a temperature approximately 50°F above that

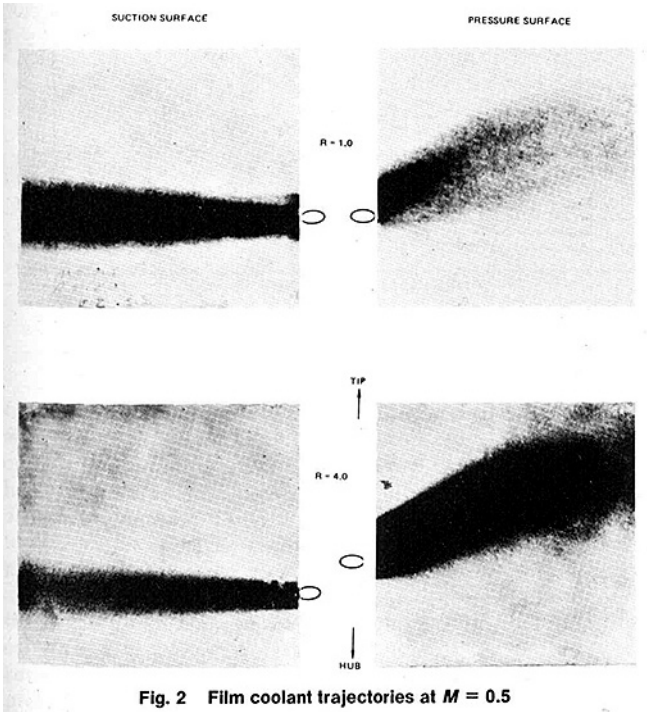

Fig. 2 Film coolant trajectories at $M = 0.5$

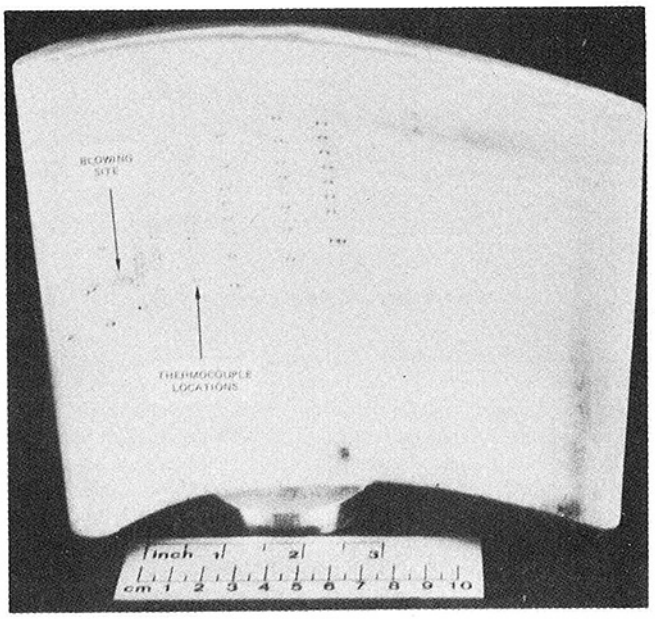

Fig. 3 Thermocouple array locations on the pressure surface

of the mainstream fluid. The *TC* lead wires from both airfoils were connected to a 144 channel *TC* scanning system mounted on the rotor (near the rig axis). The *TC* scanner communicated digitally with the rig data acquisition system computer. This digital communication eliminated all difficulties associated with slip-ring noise on analog signals.

The coolant supply system was designed to provide a coolant mixture to one blade at a time. For each flow condition, one blade was film cooled and the other blade provided a convenient and accurate station to measure the free stream adiabatic wall recovery temperature. Individual thermocouples on the film-cooled blades were calibrated by recording indicated temperatures with no cooling air flowing. All *TC* calibration corrections were less than or equal to 0.5°F.

Discussion of the Results

Typical results of the testing on the suction and pressure surfaces for twelve combinations of M and R ratios on each surface are shown in Figs. 4–7. A complete presentation of all the results is available in [10]. The figures illustrate the profiles across the film coolant footprint at each array of *TC*'s. Sketched below them are iso-effectiveness contours that have been inferred from the profiles. Several thermocouples became inoperative during the final stages of model fabrication, during installation in the rig and during testing. In total, six out of the total of 130 *TC*'s were inoperative. All of the bad *TC*'s were on the suction surface, and they have been indicated in Figs. 4 and 5. Due to this loss of instrumentation, some interpolation had to be employed in constructing the effectiveness profiles on the suction surface. In areas where this was done, the profiles have been drawn with dashed lines. The uncertainty in all measured temperatures is estimated to be 0.7°F. This can be shown by the method of [11] to result in an uncertainty in the effectiveness of at most 0.02. As a result of this the locations of the 0.02 contours, and also, but to a lesser degree, the 0.05 contours, are not considered precise. For this reason, they have been drawn in as dashed lines in all of the figures. The degree to which most of the effectiveness profiles return to zero on either side of the footprints is indicative of the uncertainty in the results.

The film cooling patterns obtained from the separate flow visualization and film effectiveness tests were consistent for all tests on both the suction and pressure surfaces. As an example, the effectiveness patterns (Figs. 4–7) can be seen to bear close resemblance to the flow visualization patterns (Fig. 2). The suction surface effectiveness footprint is narrow and has only a slight radially outward deflection. Even though the maximum effectiveness and the footprint width vary markedly over the range of M and R tested, the location of the centerline of the footprint appeared to be insensitive to these variables. As in the flow visualization tests, the pressure surface effectiveness footprint was wide and exhibited a large radial deflection. The maximum effectiveness and the footprint width on the pressure surface, however, both appear to be far less sensitive to M and R than on the suction surface.

The different widths of the suction and pressure surface coolant patterns are somewhat analogous to the differences in film coolant coverage that can be achieved through the use of compound angled blowing holes as opposed to simple streamwise blowing. Generally speaking, compound blowing can result in a much wider film coolant effectiveness footprint than simple streamwise blowing [12, 13]. On the suction surface the major axis of the cooling hole is parallel to the film coolant trace, and the result is a relatively narrow trace which is typical of simple streamwise blowing. In contrast to this, the major axis of the pressure surface hole is at an angle of approximately 30 deg to the film coolant trace, and this has produced the much wider film coolant footprint characteristic of compound blowing. As mentioned in the discussion of the flow visualization tests, it appears that the film coolant trajectory is governed primarily by the nature of the undisturbed flow over the airfoil, i.e., in the absence of film cooling. Centrifugal and Coriolis forces may be important in determining the nature of the undisturbed flow, but beyond that, they appear to have no significant impact on film coolant trajectory.

The basic conclusions of the experiment are that there is a strong radial component to the pressure surface film coolant trajectory and that both the suction and pressure surface trajectories are very insensitive to both the density ratio, R, which was varied over a range from 1 to 4 and the mass flux ratio, M, which was varied over a range from 0.5 to 1.5.

The fact that film coolant trajectory is insensitive to coolant flow conditions eliminates one of the concerns of the turbine designer. However, one must keep in mind that the pressure surface coolant

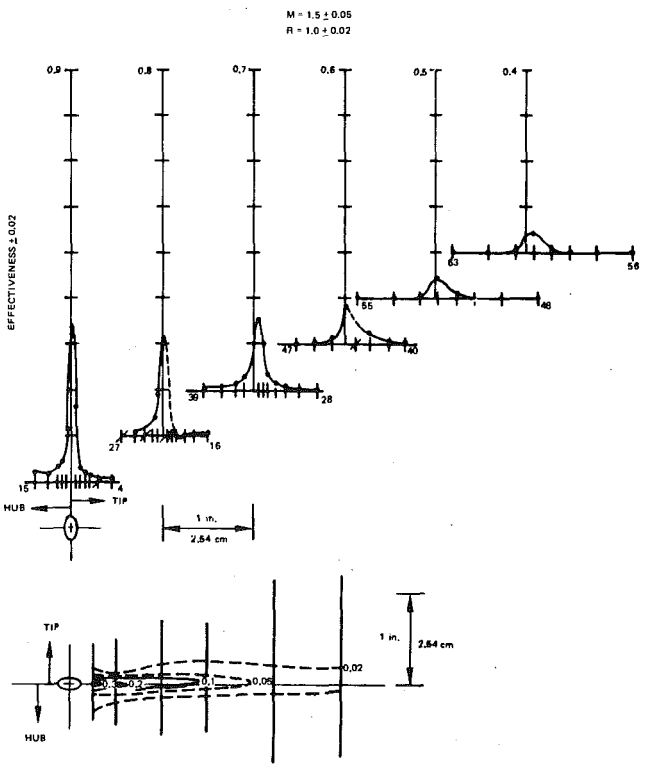

Fig. 4 Suction surface film cooling

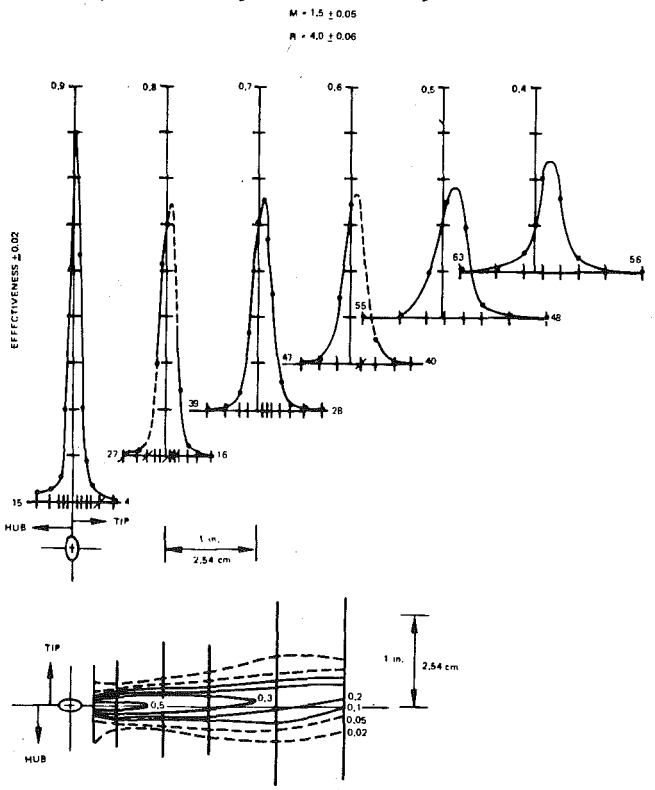

Fig. 5 Suction surface film cooling

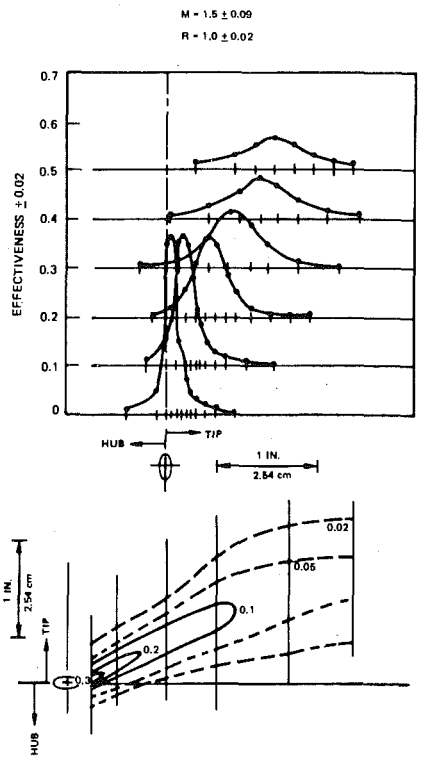

Fig. 6 Pressure surface film cooling

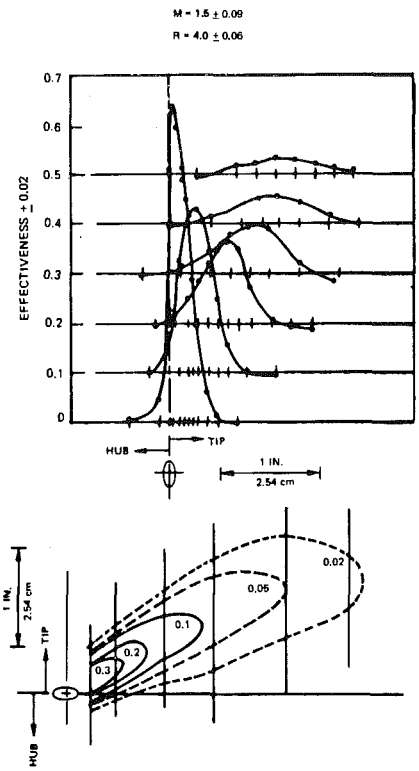

Fig. 7 Pressure surface film cooling

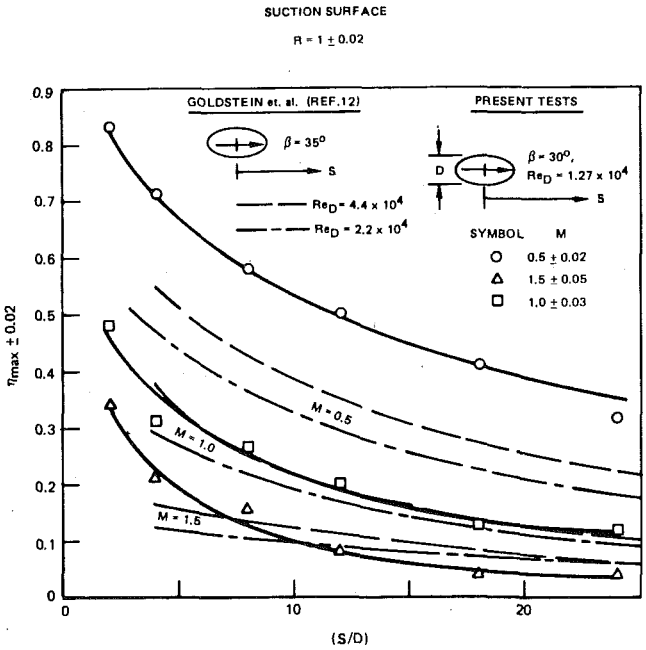

Fig. 8 Decay of maximum effectiveness

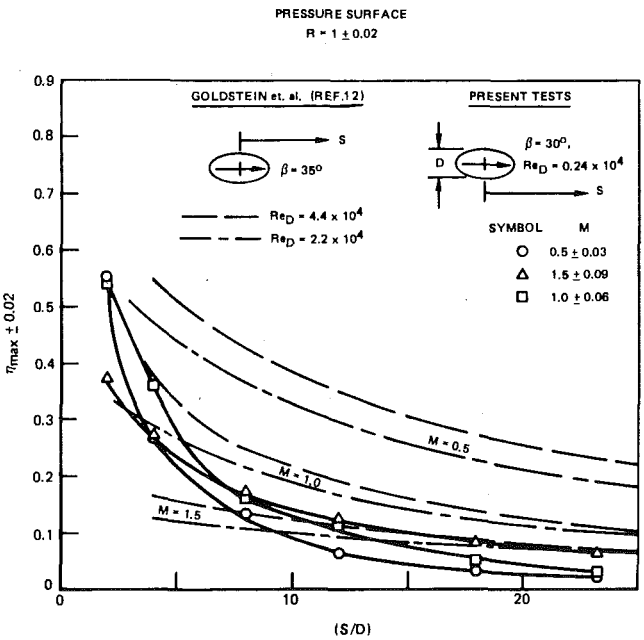

Fig. 9 Decay of maximum effectiveness

trajectory represents a wide departure from typical design system assumptions. This can give rise to two problems. First, large portions of the airfoil surface downstream (axially) of the coolant discharge hole will be starved of film coolant since this air will have moved radially outward toward the tip of the airfoil. The second problem arises in that compound angled holes are frequently used to achieve improved film cooling coverage on turbine airfoil surfaces. These holes are generally oriented under the assumption of purely axial flow on the airfoil surface. If the radial flow occurring on the blade pressure surface was aligned with the compound hole angle, the enhanced film coverage would not be achieved. The result of both of these possible problems would be burning near the airfoil pressure surface trailing edge in the region downstream of the blowing sites experiencing maximum radial flow.

The effectiveness data taken during the present program have been compared to flat plate wind tunnel data reported by Goldstein, et al. [12]. There were, however, some differences between the present film cooling test conditions and those of [12]. For the present program, the suction and pressure surface holes are at 30 deg to the surface, but in the tests of [12], the holes were at 35 deg to the surface. For the present program, the pressure and suction surface blowing site Reynolds numbers (Re_D) are 0.24×10^4 and 1.27×10^4, respectively, whereas for the tests of [12] values of 2.2×10^4 and 4.4×10^4 were employed. This difference is not believed to be important since the data of [1,

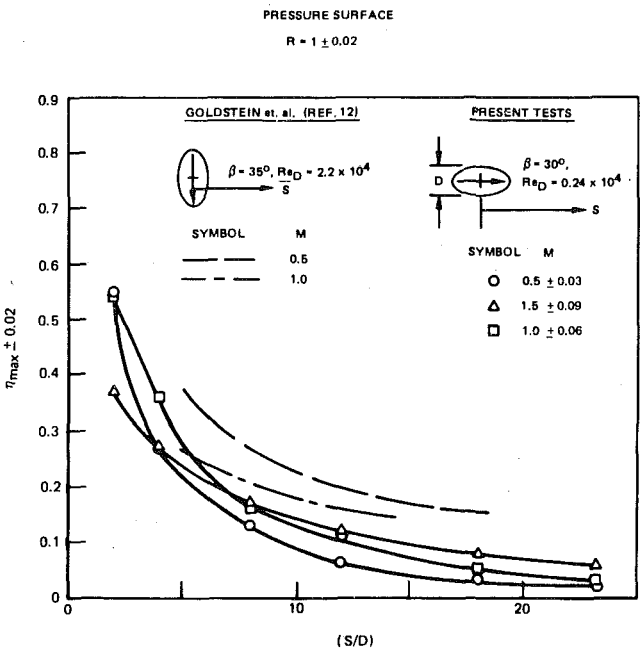

Fig. 10 Decay of maximum effectiveness

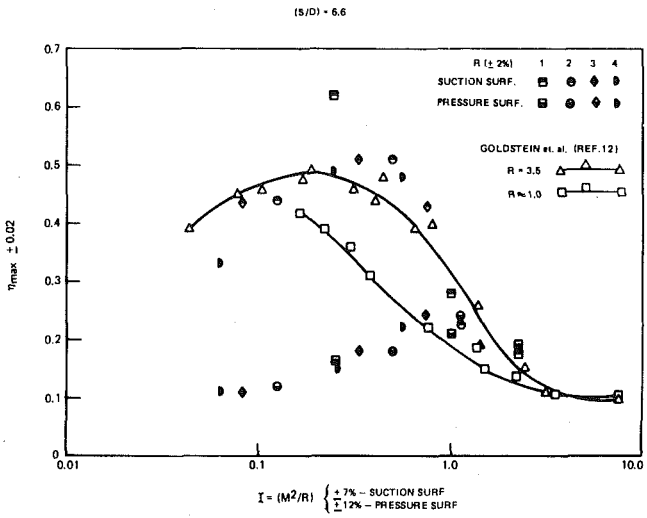

Fig. 11 Maximum effectiveness as a function of momentum flux ratio and density ratio

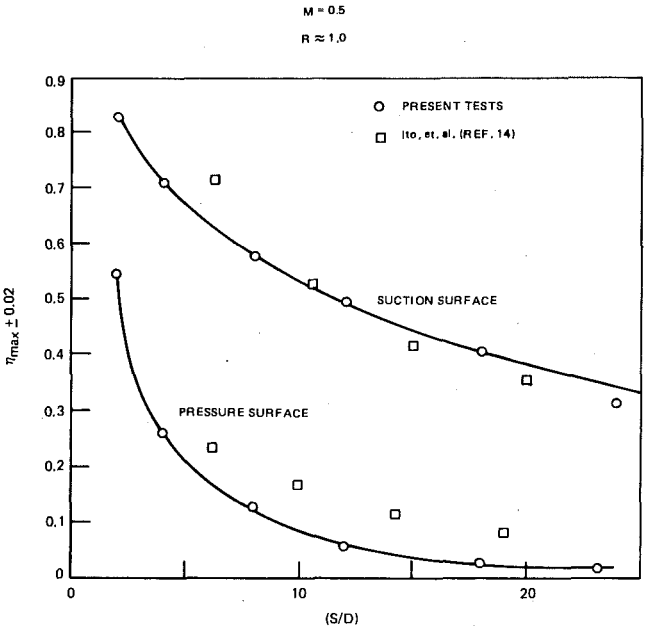

Fig. 12 Decay of maximum effectiveness

5] indicate that film effectiveness is insensitive to Reynolds number. Most of the data reported in [12] are for a normalized displacement thickness (δ^*/D) of 0.116. For the present tests, (δ^*/D) is 0.036 and 0.059 on the suction and pressure surfaces respectively. The reduced coolant injection angle and (δ^*/D) ratio of the present tests would both be expected to produce effectivenesses slightly higher than those of [12]. This generally did not turn out to be the case as shall become apparent in the following paragraphs.

The suction surface data are compared with the data of [12] in Fig. 8. For a density ratio, R, of 1.0 the decay of the maximum effectiveness is shown as a function of normalized distance aft of the center of the blowing site. For blowing rates, M, of 1.0 and 1.5, the present data are in reasonably good agreement with the data of [12]. At $M = 0.5$, there is a significant difference. The reason for this difference is unclear at present, but it may be due to the effects of curvature as shall be discussed below. The pressure surface data are compared with the same flat plate data of [12] in Fig. 9. As can be seen, significant differences exist between the two sets of data for all conditions. The effectiveness data of the present program are, in general, much lower and less sensitive to M than those of [12]. The pressure surface data, however, show a greater similarity to other data of [12] which were obtained with the hole oriented at right angles to the flow direction (Fig. 10). The lower level of maximum effectiveness and its relative insensitivity to M appear to be partially a result of the radial flow over the blowing site causing the hole to behave as a compound angled hole. A final comparison with the data of [12] is given in Fig. 11, where the maximum effectiveness is plotted as a function of the momentum flux ratio ($I = M^2/R$) at a normalized distance downstream of the hole center (S/D) of 6.6. Although the suction surface results are in reasonably good agreement with those of [12], the pressure surface results are distinctly different. The conclusion drawn from these comparisons is that although the suction surface film coolant behavior is similar in many respects to what one would have expected from the flat plate results of [12], the pressure surface results are both qualitatively different (i.e., a strong radial component to the coolant trajectory) as well as quantitatively different (i.e., the effectiveness levels are, in general, much lower than one would have expected from flat plate results).

The difference between the data presented here and those of Goldstein, et al. [12] may partially result from the effects of surface curvature. In a recent paper, Ito, et al. [14] have reported film cooling data taken on a turbine blade in a plane cascade with rows of blowing sites on both the suction and pressure surfaces. Their holes were at 35 deg to the surface and had a center-to-center distance of three diameters. In all other respects, their configuration was very similar to that of the present program. Their facility being a plane cascade, however, had no radial flow effects. Most of the data they present is laterally averaged, but some local effectiveness data is reported for a density ratio of 0.95 and a mass flux ratio of 0.5, for the pressure and suction surfaces. These data, on the hole centerlines, ([14], Figs. 4 and 5) are almost identical with those of the present program on the suction surface, and they are also quite close on the pressure surface (Fig. 12). The pressure surface effectiveness data of [14] are higher by 0.05 to 0.10 than those of the present program. This difference is probably due to both the effects of the row of holes as opposed to the single hole employed in the present program and also the effect of the radial flow. Ito, et al. [14] attribute most of the difference between suction and pressure surface film cooling behavior to the effects of surface curvature. The effects of high and low blowing rate and concave and convex surface curvature are summarized by Ito et al., in Fig. 10 of that work. This figure is for laterally averaged effectiveness, but the results it illustrates are similar in many respects to those of Fig. 11 of the present work. The high effectiveness on the suction surface at low momentum flux ratios, I, is attributed by Ito et al., to the effect of curvature causing the coolant jet to be close to the wall. At higher

values of I, the curvature effects cause the jet to lift off the surface resulting in lower effectiveness. On the pressure surface, the effects were shown in [14] to be reversed. Low values of I caused low effectivenesss, but the effectiveness increased gradually as I increased. It was suggested by Ito et al., and indeed it is confirmed by their data as well as by that of the present work (Fig. 11), that the suction (convex) and pressure (concave) surface data should cross at a value of I equal to or somewhat greater than unity.

Conclusions

Both qualitative and quantitative differences were seen to exist between the behavior of film coolant on the suction and pressure surfaces of a turbine rotor blade. On the suction surface, the film coolant had only a small radial displacement and was in many respects similar to existing data taken on flat surfaces with streamwise oriented holes. Where comparisons were possible, the suction surface data was also nearly identical with film cooling data taken by other investigators on a plane cascade airfoil of very similar geometry.

On the pressure surface, the film coolant had a large radial displacement and, in general, very low levels of effectiveness were measured. The radial displacement was a result of the radial component of the free stream flow over the blowing site. The low level of effectiveness appears to be due both to the effectively compound orientation of the hole, due to the radial flow, and surface curvature effects which tend to reduce coolant effectiveness on concave surfaces at momentum flux ratios, I, less than approximately unity.

Finally, the film coolant trajectories for each blowing site are virtually uninfluenced by the coolant blowing rate, M, and by the coolant to free stream density ratio, R.

Acknowledgments

This program was sponsored by the Air Force Aero-Propulsion Laboratory (AFSC) United States Force. The authors are indebted to the efforts of many people for the completion of this program and in particular to Mr. Charles Coffin for his skill and patience in building the models, Mr. Raymond Whitmore for developing the TC scanning system, and finally Mr. Joel Wagner and Mr. John Kostic for helping in acquiring the data.

References

1 Goldstein, R. J., "Film Cooling" in *Advances in Heat Transfer.* Academic Press, New York and London, Vol. 7, 1971, p. 321.

2 Ericksen, V. L., "Film Cooling Effectiveness and Heat Transfer with Injection Through Holes," Ph.D. Thesis, University of Minnesota, 1971.

3 Ericksen, V. L., Eckert, E. R. G., and Goldstein, R. J., "A Model for the Analysis of the Temperature Field Downstream of a Heated Jet Injected into an Isothermal Crossflow of an Angle of 90°." NASA CR72990, 1971.

4 Pedersen, D., "Effect of Density Ratio on Film Cooling Effectiveness for Injection Through a Row of Holes and for a Porous Slot," Ph.D. Thesis, University of Minnesota, 1972.

5 Liess, C., "Film Cooling with Ejection from a Row of Inclined Circular Holes, An Experimental Study for the Application to Gas Turbine Blades," von Karman Institute for Fluid Dynamics, Technical Note 97, March 1973.

6 Lander, R. D., Fish R. W., and Suo M., "External Heat Transfer Distributions on Film Cooled Turbine Vanes," *Jour. Aircraft,* Vol. 9, No. 10, Oct. 1972, pp. 707–714.

7 Muska, J. F., Fish, R. W., and Suo, M., "The Additive Nature of Film Cooling From Rows of Holes," ASME Paper No. 75-WA/GT-17, 1975.

8 Caspar, J. R., Hobbs, D. E., and Davis, R. L., "Calculation of Two-Dimensional Potential Cascade Flow Using Finite Area Methods," to be published in the *AIAA Journal,* Vol. 17, No. 12, Dec. 1979.

9 Blair, M. F. and Lander, R. D., "New Techniques for Measuring Film Cooling Effectiveness," ASME JOURNAL OF HEAT TRANSFER, Vol. 97, No. 4, Nov. 1975, pp 539–543.

10 Dring, R. P., Blair M. F., and Joslyn H. D., "Research on Centrifugal Effects on Turbine Rotor Blade Film Cooling," AFAPL (TBC), AFSC, Report No. AFAPL-TR-78-63, Aug. 1978.

11 Kline, S. J. and McClintock, F. A., "Describing Uncertainties in Single Sample Experiments," *Mech. Eng.,* Vol. 75, No. 1, 1953, pp. 3–8.

12 Goldstein, R. J., Eckert E. R. G., Eriksen, V. L., and Ramsey, J. W., "Film Cooling Following Injection Through Inclined Circular Tubes," NASA CR-72612, Nov. 1969.

13 Colloday, R. S. and Russell, L. M., "Flow Visualization of Discrete Hole Film, Cooling for Gas Turbine Applications," ASME 75-WA/HT-12, Dec. 1975.

14 Ito, S., Goldstein R. J., and Eckert, E. R. G., Film Cooling of a Gas Turbine Blade," ASME, *Journal Engineering for Power,* Vol. 100, July 1978, pp. 476–481.